JOURNAL OF OPTOELECTRONICS AND ADVANCED MATERIALS, Vol. 11, No. 4, April 2009, p. 429 - 436

Influences of copper and manganese concentrations on the properties of polycrystalline ZnS:Cu and ZnS:Mn thin films

F. GÖDE*, C. GÜMÜŞ[a]
Physics Department, University of Mehmet Akif Ersoy15030 Burdur, Turkey
[a]Physics Department, University of Çukurova 01330 Adana, Turkey

Copper and manganese doped zinc sulfide (ZnS:Cu and ZnS:Mn) thin films are deposited on glass substrates using chemical bath deposition (CBD) method, with the both copper and manganese concentration varying from 0.5 to 4 mol%. All films were annealed in the temperature range of 100-500 ºC and characterized by X-ray diffraction (XRD) and optical absorption. All samples are shown to be crystallized in the hexagonal phase of ZnS with a preferential orientation in the (008) direction. The XRD analysis showed that after annealing process, ZnS:Cu and ZnS:Mn films can be converted to ZnO:Cu and ZnO:Mn films at annealing temperature of 300 ºC. The electrical conductivity measurments were taken in the dark before and after annealing temperature of 400 ºC for 1 h. The electrical conductivity of ZnS:Cu films decreased after annealing process. However, it increased for ZnS:Mn thin films. The activation energy values were obtained using the temperature-dependent current measurements in the range of 300-623 K.

(Received January 15, 2009; accepted April 23, 2009)

Keywords: ZnS:Cu, ZnS:Mn, Thin films, XRD, Optical absorption

1. Introduction

In recent years, much effort has been devoted to the research of doped metal chalcogenide thin films. This kind of materials exhibits unusual physical and chemical properties in comparison with their bulk materials, such as size-dependent variation of the band gap energy [1]. Further more, when impurity ions doped into these structures can influence the electronic structure and transition probabilities [2].

As an important II-VI semiconductor material, ZnS is chemically more stable and technologically better than other chalcogenides (such as ZnSe), so it is considered to be a promising host material. Doped ZnS semiconductor materials have a wide range of applications in electroluminescence devices, phosphors, light emitting displays, and optical sensors. Accordingly, special attention has been paid to their luminescence properties [3]. Conventional solid state reaction [4,5], electrospinning [6], pulsed laser deposition [7], the wet chemical synthesis route [8] and chemical precipitation [9,10] have been used for the fabrication of ZnS:Cu and ZnS:Mn films.

The aim of this work is on the preparation of ZnS:Cu and ZnS:Mn thin films with varying Cu and Mn concentrations deposited onto glass substrates by CBD method. The influences of the Cu^{2+} ions and Mn^{2+} ions in the synthesis on the optical and electrical properties have been investigated before and after annealing process. Refraction index (n) has been calculated for ZnS:Cu and ZnS:Mn films. Moreover, activation energies of the hexagonal ZnS:Cu and ZnS:Mn films were calculated from the temperature-dependent current measurments. There have been many reports on how the structural and optical properties change when the ZnS films are doped and annealed, but up to now, with the incorporation of Cu^{2+} and Mn^{2+} ions into the ZnS, activation energies in the temperature range of 300-623 never reported before.

2. Experimetal details

Thin films of ZnS:Cu and ZnS:Mn were produced by chemical bath deposition method on glass substrates at 80 ºC for 6 h. To obtain ZnS:Cu thin films, first, the solution was prepared by mixing 2.5 ml of 1 M zinc acetate [Zn $(CH_3COO)_2$] and 0.1 M copper chloride ($CuCl_2$ $2H_2O$). The concentration of copper ions were adjusted by controlling the quantity of copper chloride in the above mixture, varying from 0.5 % to 4 % (in molar ratio of copper ions to zinc ions). Then, 0.5 ml of 3.75 M triethanolamine (TEA), 2.5 ml ammonia /ammonium chloride (NH_3/NH_4Cl, pH=10.55) buffer solution, 0.8 ml of 0.66 M tri-sodium citrate ($C_6H_5Na_3O_7$), 2.5 ml of 1 M thiourea were added to the reaction medium. Lastly, deionized water was added to make the total volume of the solution 20.8 ml. The mixture was poured into a beaker and heated to 80 °C. For the preparation of ZnS:Mn films, 0.1 M manganese chloride ($MnCl_2$ $2H_2O$) was used and same procedure was followed as in preparation of ZnS:Cu films.

When the deposition temperature was reached, one precleaned glass slide was introduced into the each solution which had different copper and manganese concentration and left for deposition times of 6 h. After the

glass substrates were removed, they were washed with tap water, rinsed in deionized water to remove soluble impurities and then dried in the air.

Gold (Au) contacts were made by vacuum evaporation to allow measurement of the *I-V* characteristics of the films. In order to measure the activation energies, the films were put into the oven and then heated to 623 K. During heating, the voltage was held constant at 20 V and the corresponding output current was measured by digital multimeter. The temperature-dependent current measurment of the ZnS:Cu and ZnS:Mn films were recorded in the temperature range 300-623 K.

The X-ray diffraction patterns were recorded using Rigaku Rint 2000 X-ray diffractometer with a rotating anode and a Cu-Kα_1 radiation source (λ=0.15406 nm) at 40 kV and 30 mA. Optical transmission data was obtained by Shimadzu UV-2101PC scanning spectrophotometer. The current-voltage (*I-V*) measurements were obtained using HP4140B pA meter/DC voltage source, HP34401 Model Digital multimeter and Vee One Lab 6.1 computer program. Metal contacts were obtained by vacuum evaporation using a Leybold Heraus 300 Univex. The activation energy was measured using a Netes 6303D model power supply and a Nabertherm model oven.

3. Results and discussion

3.1. Structural properties

The XRD patterns of the ZnS:Cu and ZnS:Mn thin films are shown in Fig. 1a and b respectively, reveal the hexagonal structure of ZnS [11]. Only one peak, corresponding to the (008) lattice plane of ZnS (2θ~29.32º for ZnS:Cu and 2θ~29.34º for ZnS:Mn) appears on the diffractograms. The lattice parameters *a* and *c* of the unit cell were calculated according to the following relation:

$$\frac{1}{d_{hkl}^2} = \frac{4}{3}\left(\frac{h^2 + hk + k^2}{a^2}\right) + \frac{l^2}{c^2} \qquad (1)$$

where *d* is the interplanar spacing of the atomic planes. As determined from the position of the peak (008), lattice parameters *a* and *c* for all films are estimated to be ~ 0.386 nm and ~ 2.43 nm, respectively. When they are compared with the literature which were given as 0.382 nm and 2.49 nm respectively, it can be said that calculated lattice parameters are in agreement with the literature [11].

Using the Debye-Scherer formula [12], the mean crystalline sizes calculated from the full-width at half-maximum (FWHM) of the strongest diffraction peak in the (008) direction. Fig. 2 shows the dependence of grain size with the copper and manganese concentration. It is shown that grain sizes of the ZnS:Cu and ZnS:Mn films decrease with copper concentration from ~66.8 nm to ~40.0 nm and with Mn concentration from ~64 nm to ~32 nm, respectively.

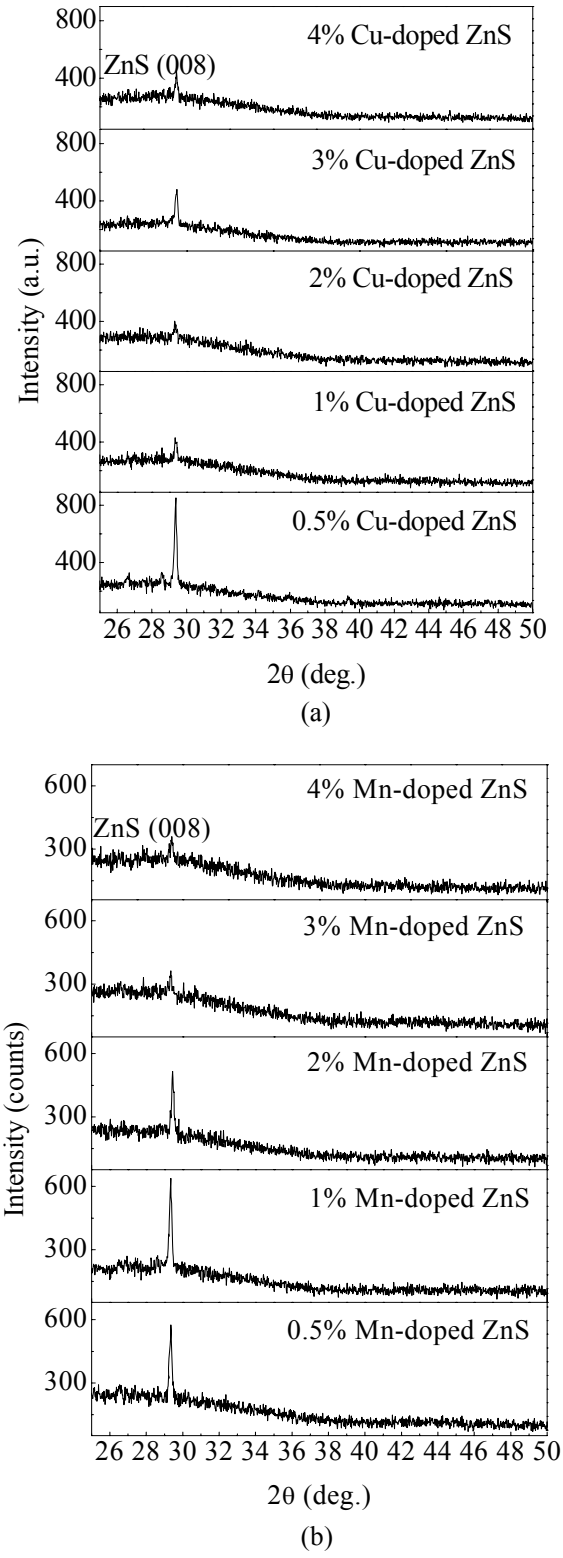

Fig. 1. XRD patterns of the (a) ZnS:Mn and (b) ZnS:Mn films with various Cu and Mn concentration.

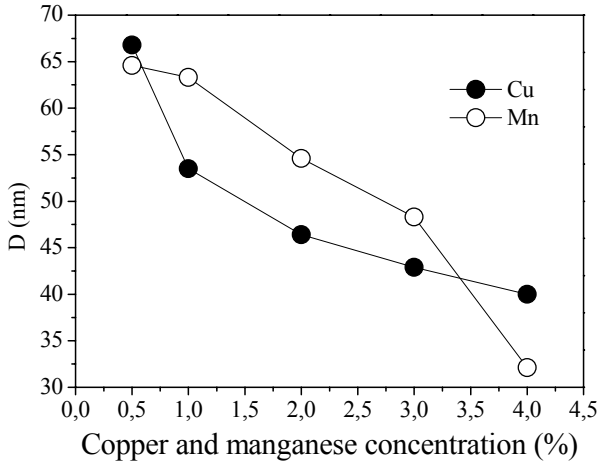

Fig. 2. The variation of the grain size (D) calculated from (008) lattice plane as a function of the Cu and Mn concentration for ZnS films deposited.

It can be clearly seen from Fig. 1 and Fig. 2 that with the incorporation of Cu^{2+} and Mn^{2+} ions into the ZnS, a reduction in the grain sizes have been occured. This reduction is not observed clearly in Ref. [13] from the XRD patterns of ZnS:Cu,Mn films with the variation of Cu concentration. Moreover in Ref. [14], while Mn and Cu concentration are increased in ZnS:Mn,Cu,Cl films, the cubic related (111) and (220) peaks are slightly decreased whereas the hexagonal-related (110) and (101) peaks are slightly increased.

As-grown films are annealed in the air at temperature range of 100-500 ºC during 1 h. Fig. 3 shows XRD patterns of the annealed films (500 ºC). It is shown in Figs. 3a and b that annealed ZnS:Cu and ZnS:Mn films have kept peak relating to ZnS with preferential orientation along the (008) and have also three peaks, which correspond to the (100), (002) and (101) planes of the hexagonal phase of ZnO [15]. In Fig. 3a and b, diffraction peak, which belongs to the (008) plane of hexagonal ZnS was slowly decreased untill Cu and Mn concentration of 3% and fully disappeared for the Cu and Mn concentration of 4%. Our results can be compared with Ref. [16] in which no diffraction peak for ZnS has been found after annealing process from the XRD results. As a result it can be said that as-grown ZnS:Cu and ZnS:Mn films are slowly transformed into hexagonal ZnO:Cu [17] and ZnO:Mn films. During the oxidation process, Zn-S bonds are slowly broken and sulfur atoms are replaced by oxygen atoms to form Zn-O bonds. Moreover there are other records on annealed ZnS [18,19] and ZnS:Cu,Ga [17] which show films turn into ZnO and ZnO:Cu,Ga films, respectively after the annealing process.

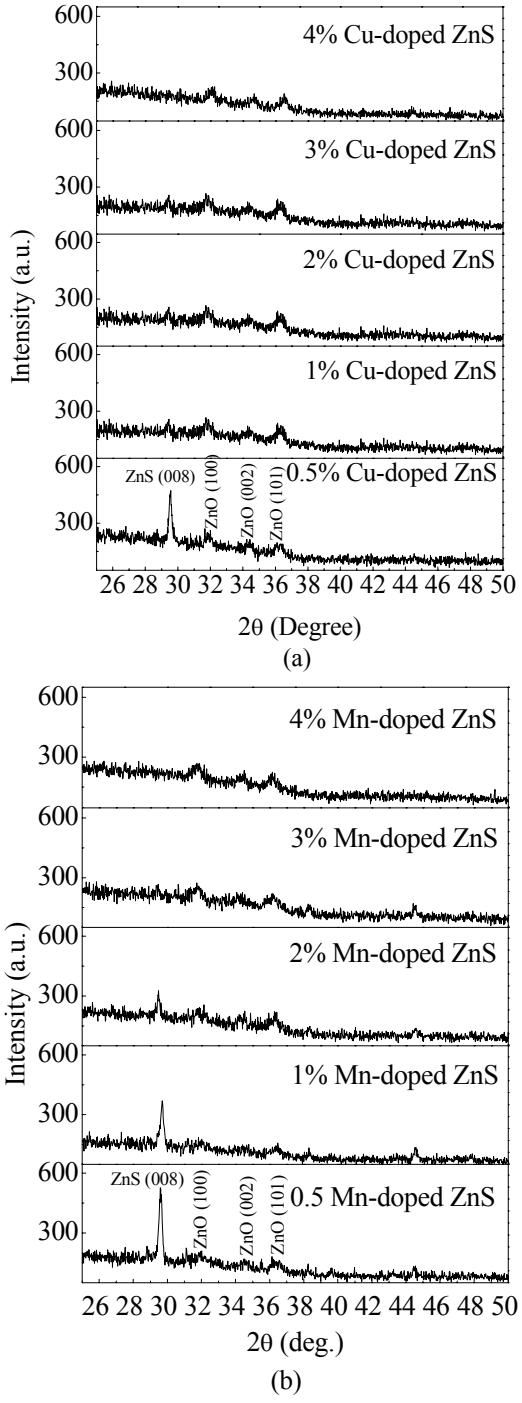

Fig. 3. XRD patterns of the (a) ZnS:Cu and (b) ZnS:Mn films annealed at 500 ºC for 1 h with various Cu and Mn concentrations.

3.2. Optical properties

The optical properties of Cu-doped and Mn-doped ZnS films are determined from transmission measurements in the wavelength range of 290-800 nm. The thicknesses of the films were calculated from the interference patterns around 400-700 nm [20]. The film thicknesses varied from 803 nm to 975 nm for ZnS:Cu films and from 892 nm to 998 nm for ZnS:Mn films. Fig. 4a and b show the transmittance spectra of Cu-doped and Mn-doped ZnS films, respectively. The optical transmission increases from 64% to 73% for ZnS:Cu films with increasing Cu concentration (Fig. 4a) and from 71% to 83% for ZnS:Mn films with increasing Mn concentration (Fig. 4b) except for Mn concentration of 2%. At this concentration optical transmission decreased to the value of 58%.

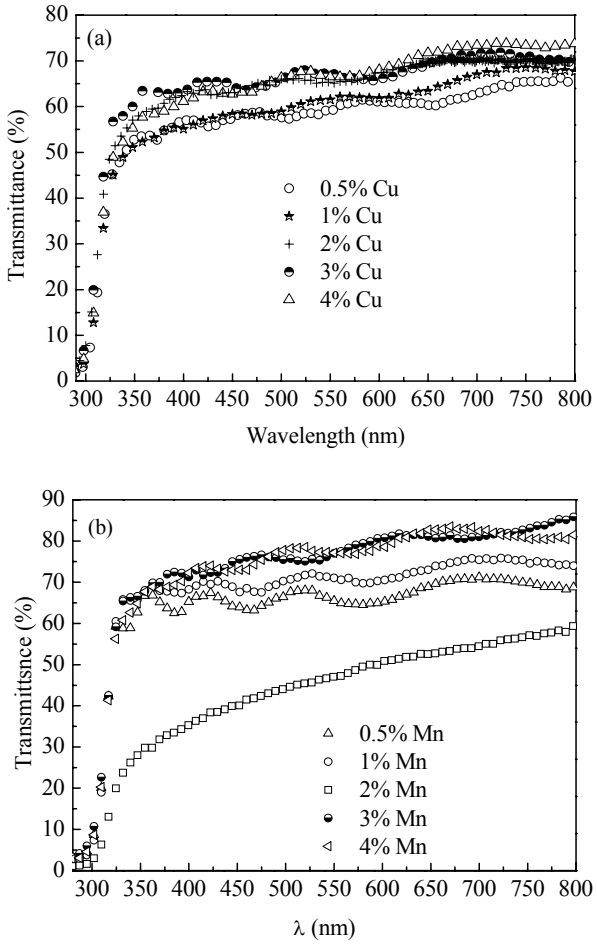

Fig. 4. Transmittance spectra of (a) ZnS:Cu and (b) ZnS:Mn films with various Cu and Mn concentrations.

The optical band gap was determined from the absorption coefficient using the relation:

$$(\alpha h\nu)^2 = K(h\nu - E_g), \qquad (2)$$

where α is the absoption coefficient, $h\nu$ is the photon energy, K is constant and E_g is the energy gap between the bottom of the conduction band and top of the valance band at the same value of wave vector. An energy band gap of ZnS:Cu film with Cu concentration of 0.5% was obtained by extrapolating the linear part of the curve $(\alpha h\nu)^2$ versus photon energy $(h\nu)$ and the result is shown in Fig. 5. The band gap values of all ZnS:Cu and ZnS:Mn films are listed in Table 1. The band gap value of ZnS:Cu film increased from 3.95 eV to 3.98 eV with increasing Cu concentration. For the ZnS:Mn films, fisrt, it decreased from 3.94 eV to 3.84 eV with increasing Mn concentration from 0.5% to 2% and then it increased to the value of 3.95 eV untill the Mn concentration of 4%. These results are comparable with Ref. [21] in which band gap decreased with increasing Cu concentration.

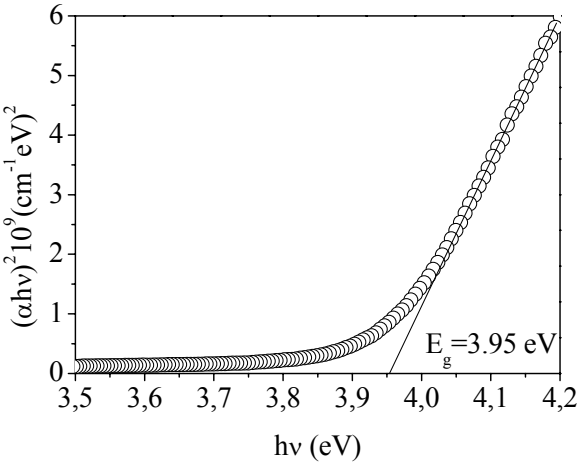

Fig. 5. Plot of $(\alpha h\nu)^2$ versus photon energy $(h\nu)$ for ZnS:Cu film with Cu concentration of 0.5%..

Table 1. The band gap values of ZnS:Cu and ZnS:Mn films with various Cu and Mn concentration

Cu or Mn (%)	ZnS:Cu, E_g (eV)	ZnS:Mn, E_g (eV)
0.5	3.95	3.94
1	3.95	3.87
2	3.95	3.84
3	3.95	3.93
4	3.98	3.95

Annealing temperature has an important effect on the transmittance and the absorption edge. As the annealing temperature increases, the absorption edge gradually shifts toward the longer wavelengths, causing the band-gap shrinkage. As-grown ZnS:Cu and ZnS:Mn films were annealed at 100 ºC, 200 ºC, 300 ºC, 400 ºC and 500 ºC for 1 h in the air. The band gap values of all annealed ZnS:Cu films (Fig. 6a) and all ZnS:Mn films (Fig. 6b) decreased with annealing temparures. It is shown from figures 6a and

6b that, all ZnS:Cu and ZnS:Mn films turn into ZnO:Cu and ZnO:Mn films at annealing temperature of 300 ºC [17].

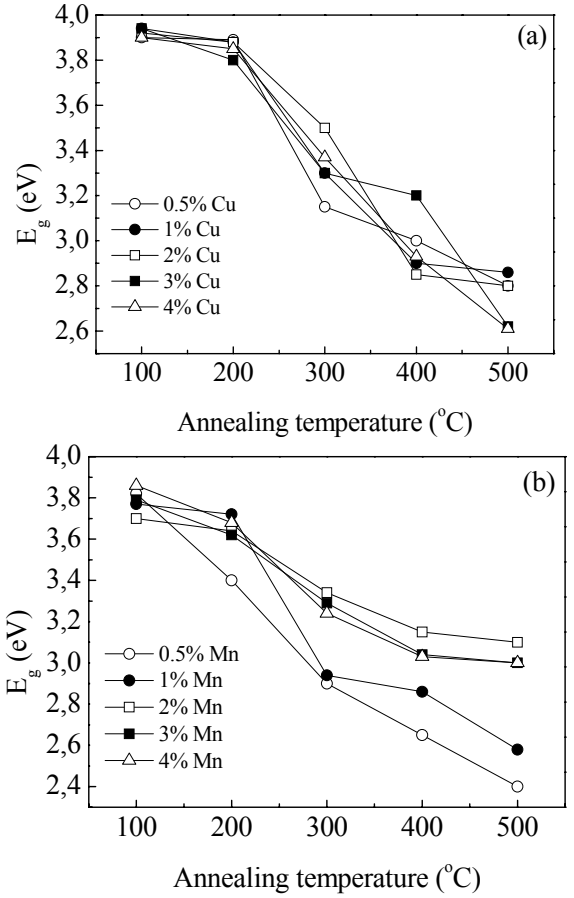

Fig. 6. The dependence of band gap values of (a) ZnS:Cu and (b) ZnS:Mn films on annealing temperatures.

The refractive index n is a very important physical parameter related to the microscopic atomic interactions. The refractive index (n) values of the ZnS:Cu (Fig. 7a) and ZnS:Mn (Fig. 7b) films were calculated from absorbance (A), absoption coefficient (α) transmittance (T) and reflection (R) spectra by using the equations given below [22,23]:

$$T = 10^{-A}, \tag{3}$$

$$\mathrm{I} = (1-\mathrm{R})^2(\mathrm{I_o e^{-\alpha d}}), \tag{4}$$

$$\alpha = \frac{\mathrm{A}}{\mathrm{d}}, \tag{5}$$

$$k = \frac{\alpha\lambda}{4\pi}, \tag{6}$$

$$n = \frac{1+R}{1-R} + \sqrt{\frac{4R}{(1-R)^2} - k^2}, \tag{7}$$

where A is the absorbance, d is the thickness of the film, I_o and I are the intensities of the incident and transmitted light respectively.

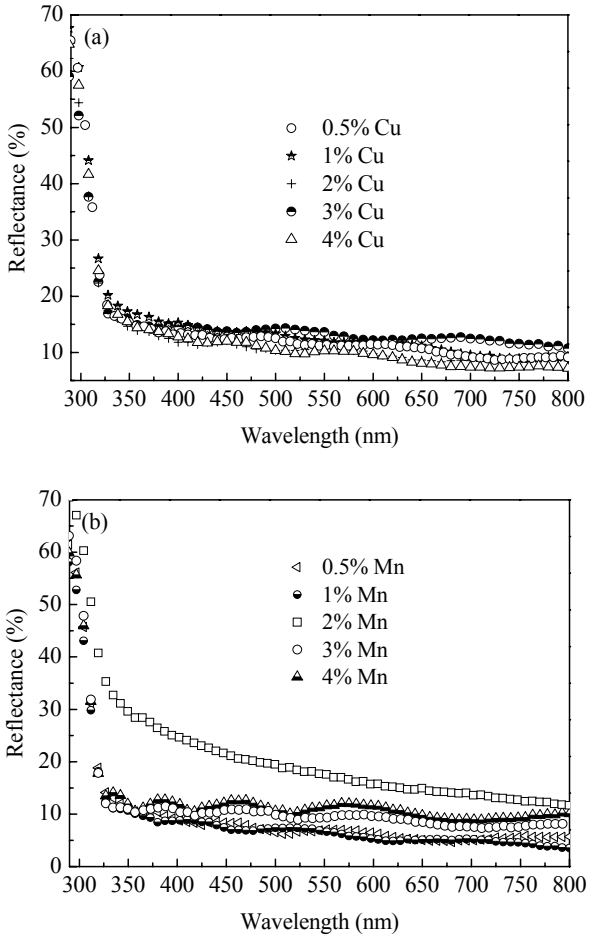

Fig. 7. Reflectance spectra of (a) ZnS:Cu and (b) ZnS:Mn films with various Cu and Mn concentrations.

The dependence of the refractive index on the Cu and Mn concentrations are shown in Fig. 8. The refractive index of both ZnS:Cu and ZnS:Mn films increase presumably due to the increase of film density with increasing Cu and Mn concentrations. The dependence of refractive index on the film density could be easily explained by the well known Clausius–Mossotti relation [25,26]. The refractive index values are comparable with our previous work for undoped ZnS [24] in which it was obtained as 2.05 at wavelength of 550 nm.

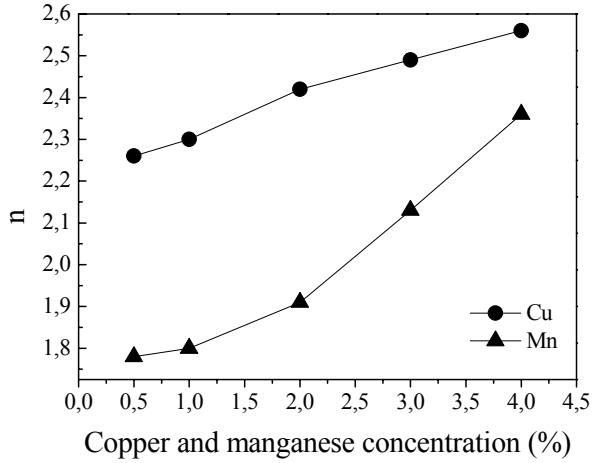

Fig. 8. The variation of refractive index of ZnS:Cu and ZnS:Mn films with various Cu and Mn cocentrations obtained at wavelength of 550 nm.

3.3. Electrical properties

I-V characteristics of the ZnS:Cu and ZnS:Mn films before and after annealing at 400 ºC for 1 h were obtained. Surface type (planar) Au contacts were made for electrical measurements. The current values of the films were measured at room temperature and in the dark by applying voltage values between 1 and 100 V. The *I-V* variations of all films are linear. Thus, the ohmic current mechanism is dominant for as-grown and annealed ZnS:Cu and ZnS:Mn films because of the current relationship to voltage were in the form of $I \sim V^{1.00}$ and ohmic conduction were dominant for the voltage range of 1 - 100 V [20]. The electrical conductivities of the films were calculated using Ohm's law given by:

$$J = \sigma E, \tag{8}$$

where J is the electric current density, (σ) is the electrical conductivity and E is the electric field. Fig. 9 shows the *I-V* characteristic of as-grown and annealed ZnS:Cu films. The electrical conductivitit of as-grown ZnS:Cu films is found in the range of 1.00×10^{-8} $(\Omega.cm)^{-1}$-4.43×10^{-10} $(\Omega.cm)^{-1}$ and it decreases nearly with increasing Cu concentration. When the films are annealed at 400 º for 1 h, the electrical conductivity of ZnS:Cu films was decreased by about two order of magnitude for the Cu concentration of 0.5% and 2%. However, for the Cu concentration of 3%, it was increased by about one order of magnitude while for Cu concentration of 4 % didn't have a large effect on the order of magnitude of the electrical conductivity (Table 2). For the as-grown ZnS:Mn films except Mn concentration of 2%, the electrical conductivity values are found in the order of ~10^{-10} while Mn concentration of 2%, it is in the order of 10^{-9} (Table 2). The electrical conductivity values are consistent with the literature values [24,27].

Table 2. The electrical conductivity values of as-grown and annealed ZnS:Cu and ZnS:Mn films with various Cu and Mn concentrations.

Cu or Mn (%)	ZnS:Cu, σ $(\Omega.cm)^{-1}$		ZnS:Mn, σ $(\Omega.cm)^{-1}$	
	As-grown	Annealed	As-grown	Annealed
0.5	1.00×10^{-8}	8.50×10^{-10}	4.32×10^{-10}	4.18×10^{-9}
1	3.32×10^{-10}	2.46×10^{-10}	3.86×10^{-10}	8.97×10^{-9}
2	4.70×10^{-9}	9.50×10^{-11}	1.91×10^{-9}	2.28×10^{-8}
3	4.00×10^{-10}	1.66×10^{-9}	2.91×10^{-10}	9.33×10^{-9}
4	4.43×10^{-10}	9.15×10^{-10}	6.84×10^{-10}	2.09×10^{-9}

A reduction in electrical conductivity for ZnS:Cu films with Cu concentration of 0.5% and 2% is attributed to the surface tension [28] due to substitution of Cu ions with Zn ions causing electroneutral defects [29]. Moreover decreasing in electrical conductivity after annealing process is ascribed to the increasing of lattice defects and dislocations of the films [30,31].

On the other hand, an increase in electrical conductivity for ZnS:Mn films with annealing is due to the improvment of oxygen vacancies in ZnS:Mn lattice [32,33]. Different oxygen partial pressure controls the metal interstitials and oxygen deficiencies in the lattice, which leads to crystal defect, and the defect chemistry plays an important role for the increase in the electrical conductivity of the ZnS:Mn films.

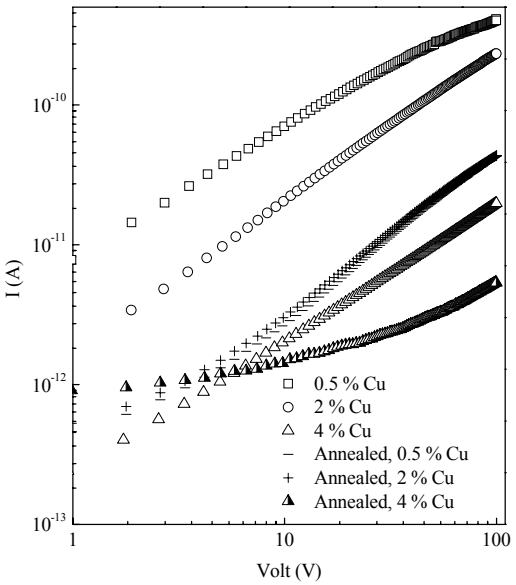

Fig. 9. The I-V characteristics of as-grown and annealed ZnS:Cu films.

The activation energies of the films were obtained using the following equation:

$$I = I_0 \exp\left(\frac{-E_a}{kT}\right), \tag{9}$$

where I is the current, E_a is the activation energy k is the Boltzman constant and T is the annealing temperature. In order to calculate the activation energies, ZnS:Cu and ZnS:Mn films were heated in the oven by raising the temperature from 300 K to 623 K. The graphical representetion of $ln(I/I_0)$ versus 1000/T for ZnS film with varied copper concentration is given in Fig. 10. The plot of the logarithm of the current flow against $1000/T$ yields a straight line with a slope of $-E_a/k$. All activation energies were calculated by using this procedure.

The temperature dependence current measurments can be divided (Fig. 10) into three regions (I, II and III) seperated by dashed lines in the temperature range from 300 to 623 K. These regions arise from different conduction processes. Calculated activation energy values for these regions are given in Table 3 for all ZnS:Cu and Zns:Mn films. The activation energy value of E_1 could be attributed to shallow trap levels while activation energies which are related with E_2 and E_3 might be ascribed to deep and deeper trap levels, respectively. Introduced of Cu^{2+} and Mn^{2+} ions into the ZnS (Cu or Mn substitutes for Zn as Cu^{2+} or Mn^{2+}) produces deep or deeper acceptor level in ZnS.

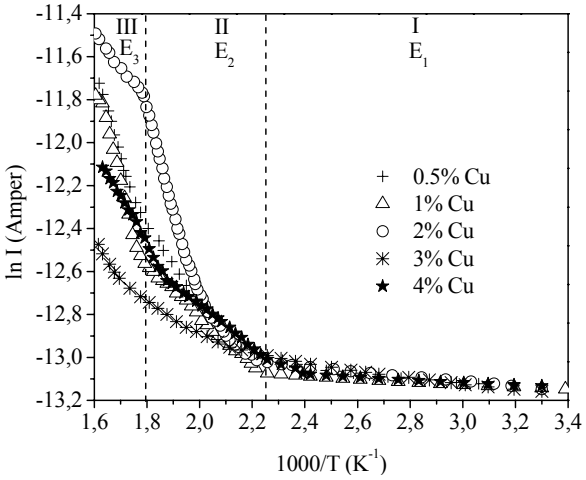

Fig. 10. The lnI versus 1000/T graphs of ZnS:Cu films deposited at 80 ºC for 6 h.

Table 3. Activation energy values of ZnS:Cu and ZnS:Mn films deposited at 80 ºC for 6 h.

Cu or Mn (%)	ZnS:Cu, Activation energy (eV)			ZnS:Mn, Activation energy (eV)		
	E_1	E_2	E_3	E_1	E_2	E_3
0.5	0.008	0.148	0.370	0.10	0.22	0.48
1	0.006	0.098	0.455	0.09	0.11	0.58
2	0.010	0.396	0.133	0.05	0.16	0.47
3	0.013	0.050	0.093	0.10	0.23	0.51
4	0.005	0.829	0.189	0.01	0.15	0.38

4. Conclusions

The effect of Cu or Mn doping varying from 0.5 % to 4 % (in molar ratio of copper ions to zinc ions) on the structural, optical and electrical properties of ZnS films has been investigated. The X-ray diffraction results show that all films have wurtzite phase of ZnS and the grain sizes of ZnS:Cu and ZnS:Mn films decrease with the incorporation of Cu^{2+} and Mn^{2+} ions into the ZnS lattice. The transmission improves with the increasing Cu and Mn concentration. After annealing process ZnS:Cu and ZnS:Mn films turn into the ZnO:Cu and ZnS:Mn films at annealing temperature of 300 ºC. The refractive index of the film was found to increase with the increasing Cu and Mn concentrations at a wavelength of 550. The electrical conductivity of the ZnS:Cu films lies in the range 10^{-8}-10^{-10} $(\Omega.cm)^{-1}$ and decreased by about two order of magnitude for the Cu concentration of 0.5% and 2%. The electrical conductivity of the ZnS:Mn films was ontained in the range 10^{-9}-10^{-10} $(\Omega.cm)^{-1}$. It can be concluded from the investigations that Cu and Mn cocentration have strong influence on the structural, optical and electrical properties of ZnS films, and ZnS:Cu and ZnS:Mn films can be suitable materials for optoelectronic applications because of high electrical conductivity and transmission.

References

[1] W. Chen, J.-O. Malm, V. Zwiller, Y. Huang, S. Liu, R. Wallenberg, J.-O. Bovin, L. Samuelson, Phys. Rev. B **61**, 1021 (2000).
[2] Y. L. Soo, Z. H. Ming, S. W. Huang, Y. H. Kao, R. N. Bhargava, D. Gallagher, Phys. Rev. B **50**, 7602 (1994).
[3] W. Q. Peng, G. W. Cong, S. C. Qu, Z. G. Wang, Opt. Mater. **29**, 313 (2006).
[4] Wendeng Wang, Fuqiang Huang, Yujuan Xia, Anbao Wang, J. Lumin. **128**, 190 (2008).
[5] Wendeng Wang, Fuqiang Huang, Yujuan Xia, Anbao Wang, Jianhua Yang, Mater. Res. Bull. **43**, 1892 (2008).
[6] Haiying Wang, Xiaofeng Lu, Yiyang Zhao, Ce Wang, Mater. Lett. **60,** 2480 (2006).
[7] K.T. Hillie, S.S. Basson, H.C. Swart, Appl. Surf. Sci. **187**, 137 (2002).

[8] Santa Chawla, N. Karar, Harish Chander, Superlattices Microst. **43**, 132 (2008).
[9] P. Yang, C. Song, M. Lü, G. Zhou, Z. Yang, D. Xu, D. Yuan, J. Phys.Chem. Solid. **63**, 639 (2002).
[10] K. Manzoor, V. Aditya, S.R. Vadera, N. Kumar, T. R. N. Kutty, Appl. Surf. Sci. **252**, 3968 (2006).
[11] PDF card no :39-1363.
[12] B. D. Cullity, S. R. Stock Elements of X-ray Diffraction,, Prentice-Hall, Pearson, 2001.
[13] Wendeng Wang, Fuqiang Huang, Yujuan Xia, Anbao Wang, J. Lumin. **128**, 610 (2008).
[14] J. H. Park, S. H. Lee, J. S. Kim, A. K. Kwon, H. L. Park, S. D. Han, J. Lumin. **126**, 566 (2007).
[15] PDF card no: 36-1451.
[16] S. Wang, G. Xia, J. Shao, Z. Fan, J. Alloy. Compd. **424**, 304 (2006).
[17] T.G. Kryshtab, V. S. Khomchenko, V. P. Papusha, M. O. Mazin, Yu. A. Tzyrkunov, Thin Solid Films **403-404,** 76 (2002).
[18] X. T. Zhang, Y. C. Liu, Z. Z. Zhi, J. Y. Zhang, Y. M. Lu, W. Xu, D. Z. Shen, G. Z. Zhong, X. W. Fan, X. G. Kong, J. Cryst. Growth **240**, 463 (2002).
[19] E. J. Ibanga, C. L. Luyer, J. Mugnier, Mater. Chem. Phys. **80**, 490 (2003).
[20] F. Göde, C. Gümüş, M. Zor, J. Cryst. Growth **299**, 136 (2007).
[21] S.S. Manoharan, S. Goyal, M.L. Rao, M. S. Nair, A. Pradhan, Mater. Res. Bull. **36**, 1039 (2001).
[22] H. Kim, A. Pique, J. S. Horwitz, H. Murata, Z. H. Kafafi, C. M. Gilmore, D. B. Chrisey, Thin Solid Films **377-378**, 798 (2000).
[23] S. H. Brewer, S. Franzen, J. Alloys Compounds **338**, 73 (2002).
[24] F. Göde, C. Gümüş, M. Zor, J. Optoelectron. Adv. Mater. **9**(7), 2186 (2007).
[25] Kittel, Solid State Physics, John Wiley & Sons, New York, 1971.
[26] W. Heitman, Thin Solid Films **5**, 61 (1970).
[27] C. Elbaum, Phys. Rev. Lett. **32**(7), 376 (1974).
[28] I. Taniguchi, T. Hosokawa, J. Alloys Compounds **460**, 464 (2008).
[29] K. Lott, M. Raukas, A. Vishnjakov, A. Grebennik, J. Cryst. Growth **197**, 489 (1999).
[30] R. K. Nkum, A. A. Adimado, H. Totoe, Mater. Sci. Eng. B **55**, 102 (1998).
[31] R. Jeyakumar, S. T. Lakshmikumar, A. C. Rastogi, Vacuum **55**, 71 (1999).
[32] S. Cruz, G. Torres-Delgado, R. Castanedo-Perez, S. Jiménez-Sandoval, O. Jiménez-Sandoval, C.I. Zúñiga-Romero, J. Márquez Marín, O. Zelaya-Angel, Thin Solid Films **493**, 83 (2005).
[33] B. Saha, R. Thapa, K.K. Chattopadhyay, Sol. Energy Mater. Sol. Cells **92**, 1077 (2008).

*Corresponding author: ftmgode@gmail.com